Stability and metastability of clusters in a reactive atmosphere: theoretical evidence for unexpected stoichiometries of Mg_MO_x

Saswata Bhattacharya, Sergey V. Levchenko, Luca M. Ghiringhelli, and Matthias Scheffler
Fritz-Haber-Institut der Max-Planck-Gesellschaft, Faradayweg 4-6, D-14195 Berlin, Germany
(Dated: April 18, 2013)

By applying a genetic algorithm in a cascade approach of increasing accuracy, we calculate the composition and structure of Mg_MO_x clusters at realistic temperatures and oxygen pressures. The stable and metastable systems are identified by *ab initio* atomistic thermodynamics. We find that small clusters ($M \lesssim 5$) are in thermodynamic equilibrium when $x > M$. The non-stoichiometric clusters exhibit peculiar magnetic behavior, suggesting the possibility of tuning magnetic properties by changing environmental pressure and temperature conditions. Furthermore, we show that density-functional theory (DFT) with a hybrid exchange-correlation (xc) functional is needed for predicting accurate phase diagrams of metal-oxide clusters. Neither a (sophisticated) force field nor DFT with (semi)local xc functionals are sufficient for even a qualitative prediction.

Keywords: Clusters, *Ab initio* Atomistic Thermodynamics, Genetic Algorithm, DFT, Magnesium Oxide, Replica-exchange Molecular Dynamics

In the search for novel functional materials, atomic (sub)nanometer clusters are widely studied as model systems exhibiting unique size-dependent properties often even qualitatively different from bulk materials. For example, small clusters may exhibit completely new local structures, stoichiometries, electronic and magnetic properties unknown in the bulk materials [1]. Heterogeneous catalysis is just one important example where all mentioned issues are of fundamental importance [2–8].

The composition and structure of clusters are determined by thermodynamics and kinetics at the relevant temperature (T) and the nature of the environment. In thermodynamic equilibrium, only structures and *compositions* that minimize the free energy of the combined gas+cluster system will be stable. Although a system is often not in thermodynamic equilibrium, thermodynamic phase diagrams serve as guidelines and important limits for predicting properties and functions of real materials. In this Letter, we address the issue of stability and metastability using a model system that is relevant for many practical applications: free metal (Mg) clusters in an oxygen atmosphere.

Most of the previous research on clusters focused on properties of stoichiometric $(MgO)_M$ clusters [7, 9–15], and only few attempts have been made to study properties of the non-stoichiometric $[Mg_MO_x]$ clusters. [8–10] However, the decisive issue of stability and metastability of clusters with different compositions at realistic conditions (exchange of atoms with an environment) has not been addressed so far.

We consider a wide range of Mg_MO_x cluster sizes: $1 \leq M \leq 10$ and x determined by thermal equilibrium with the environment at given temperature T and partial oxygen pressure p_{O_2}. For each stoichiometry, the energy is minimized with respect to both geometry *and spin state*. Very unexpectedly, our results reveal (see Fig. 1) that non-stoichiometric clusters with $x > M$ are more stable at realistic (T, p_{O_2}) when $M \lesssim 5$. For bigger clusters the stoichiometric composition, $(MgO)_M$, is preferred, although with geometries very different from the bulk rock-salt structure.

For reliable determination of low-energy structures, we have developed a massively-parallel genetic algorithm (GA). GA mimics the process of "natural" selection to evolve a set of atomic structures until the structures that fit best chosen selection criteria are found [16–18]. In this work, we search for structures that minimize the DFT total energy within each stoichiometry. Details of the implementation and validation of our GA scheme are given in Ref. [19]. It is based on an initial pre-screening of structures obtained by a GA performed with a (reactive) force field (FF-GA). The approach proceeds in terms of a cascade in which successive GA runs employ higher levels of theory, with each next level using information obtained at the lower level. We also note that the method is massively-parallel: new structures are generated by combining two structures randomly selected from the running pool, via a set of modified cut-and-splice operators [19, 20] by many parallel processes (replicas), each replica optimizes its newly generated structure, and a pool of structures shared among all the replicas is updated each time a replica finds a new optimized structure. With the communication limited only to writing to / reading from the shared pool of structures, one can then run as many parallel replicas as CPU availability permits.

The free energy as a function of T and p_{O_2} is calculated for the minimum of the potential-energy surface (global minimum, GM) and (energetically) adjacent local energy minima for each stoichiometry using the *ab initio* atomistic thermodynamics (*ai*AT) approach [21–24], recently extended to cluster systems [25]. The thermodynamic phase diagram is then constructed by selecting cluster compositions and structures with the lowest free energy as a function of (T, p_{O_2}).

The set of highest binding-energy structures (within

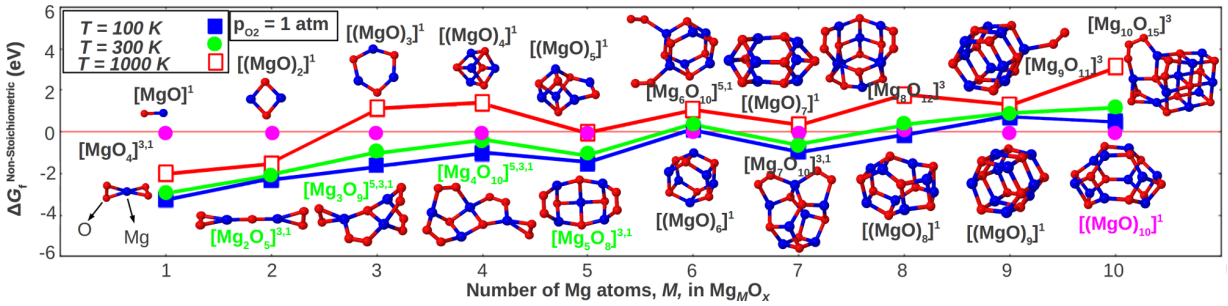

FIG. 1: Free energy of formation of thermodynamically most stable non-stoichiometric (Mg_MO_x with $M \neq x$) relative to stoichiometric ($M = x$, denoted as $(MgO)_M$) clusters at $p_{O_2} = 1$ atm and various temperatures. The geometries were optimized with PBE+vdW, and the electronic energy was calculated using PBE0+vdW. The global-minimum structures and spin multiplicity $\mathcal{M}$ (indicated as exponents to the chemical formula of the clusters, if different spin states coexist) at $T = 300$ K are also shown. Structures with chemical formulas in green are the most stable at that size M at $T = 300$ K, but other stoichiometries coexist within $2k_BT$ (i.e., the minimum concentration of clusters of a given competing type is at least 10% of the total mixture). At other temperatures, the most stable stoichiometry and/or isomer may differ from the one at $T = 300$ K. The structure labeled in magenta, $(MgO)_{10}$, is present as three coexisting isomers (the one shown is the most stable, more details can be found in Ref. 19). Coordinates for all structures are available in the Suppl. Material.

4 eV from the GM) obtained from FF-GA is used as initial pool for a DFT-based GA structure search. In this way, the initial pool contains ~ 30 structures for a small system like Mg_2O_2 and ~ 300 for the largest system we report here, $Mg_{10}O_{15}$. We label this linked approach as FF/DFT-GA. Starting from FF-relaxed structures, rather than from initial random structures, greatly reduces the overall computational time of the procedure (up to a factor of ten for our systems). This is because the geometry optimization of structures at the DFT level is computationally the most expensive part of an *ab initio* GA. A FF-GA search risks however to introduce a bias that would affect the results obtained via FF/DFT-GA. We checked [19] that this is not the case for the chosen force field (reaxFF [26, 27]), by verifying that (expensive) DFT-GA runs, i.e., started from randomly generated pools, yielded *exactly* the same final list of isomers obtained through a (much less expensive) FF/DFT-GA. It must be stressed that just locally relaxing via DFT the structures found by the FF-GA is insufficient for an accurate sampling of the DFT PES, especially at large O_2 coverages. In fact, we observed that by adopting this latter procedure one can miss some low-energy isomers [19].

A challenging problem of any GA is to guarantee that the lowest-energy structure found by the algorithm is indeed the GM. We address this problem by applying replica-exchange molecular dynamics (REMD) [25, 28, 29], a (computationally very expensive) reference method that explores the PES using the dynamics of the system at different temperatures simultaneously, and is exhaustive if the system is ergodic. Our implementation of GA gives indeed the same GM as REMD [19].

Within DFT-GA, the actual "cascade" unfolds at the local optimization step, which is initially performed with lower-level (computationally relatively cheap) numerical settings. Next, structures that are not previously found (details on the comparison of structures are given in Ref. [19]) and have energies within 2.5 eV from the current GM candidate, are further relaxed using higher-level settings [30]. All DFT calculations have been performed with the FHI-aims package [31]. For the lower-level energy minimization, the van-der-Waals (vdW)-corrected [32] PBE [33] xc functional (PBE+vdW) and "light" numerical settings with (numeric atom-centered) basis-functions set "tier 1" were used [31], and forces were converged to better than 10^{-3} eV/Å. At the higher level, energy minimization is performed with PBE+vdW functional, "tight - tier 2" settings, and forces were converged to better than 10^{-5} eV/Å. The energy of these further optimized structures are evaluated via vdW-corrected [32] PBE0 [34] hybrid xc functional (PBE0+vdW), with "tight - tier 2" settings [35]. Within DFT-GA, the latter energy is used to evaluate the fitness function, i.e., [19] a mapping of the energy interval between highest- and lowest-energy cluster in the running pool into the interval $[0, 1]$. The higher the value of the fitness function for a cluster, the higher is the probability of selecting it for generating a new structure.

It has been recently shown [36] that HSE06 functional [37] yields a good description of the level alignment and electron transfer in MgO. Based on comparison for selected clusters, we find that PBE0, which belongs to the same family of functionals, yields formation energies essentially identical to HSE06 (within 0.05 eV for Mg_MO_x neutral clusters, see also [19]) The accuracy of PBE0+vdW energies for Mg_MO_x clusters was also validated against the highest level currently achievable within the DFT framework, i.e., the renormalized second-order perturbation theory (rPT2) [38], here applied on PBE orbitals (rPT2@PBE) [39].

We find that PBE+vdW strongly overestimates stability of clusters with larger x, resulting in a qualita-

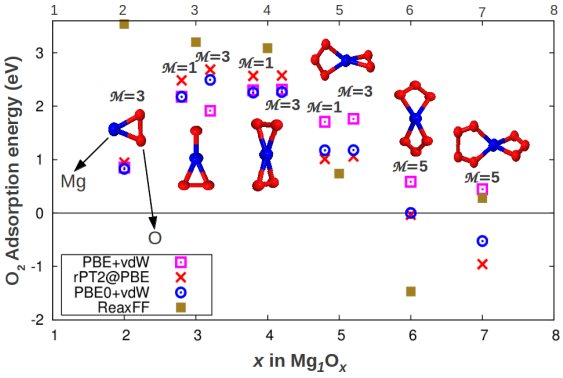

FIG. 2: Energy of O_2-adsorption on MgO_x clusters (energy of the reaction $MgO_x + O_2 \rightarrow MgO_{x+2}$ calculated at the PBE+vdW GM geometry) calculated with different xc functionals and reaxFF [26]. For the cases where singlet (S) and triplet (T) spin states are almost degenerate, the two sets of energies are shown (for DFT only, since ReaxFF does not describe spin). In these cases, the spin state of MgO_x is chosen to be singlet for triplet MgO_{x+2}, and triplet for singlet MgO_{x+2}, to preserve the spin-conservation rule (O_2 is always kept in its ground triplet electronic state). The geometry differences of clusters with different spin states are invisible at this scale.

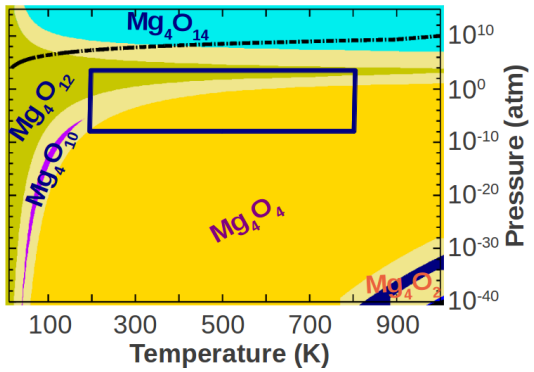

FIG. 3: Phase diagram for Mg_4O_x clusters in an oxygen atmosphere. The geometries are optimized with PBE+vdW and the total energies are calculated with PBE0+vdW. The sand-colored unlabeled areas are regions where different compositions (at least the adjacent ones) coexist (see text). The thick black line is the O-rich limit [19, 23, 24]: Above this line, O_2 droplets condensate on the clusters. The rectangle encompasses a region accessible to experiments.

tively incorrect prediction that O_2 adsorption would be favored over desorption up to a large excess of oxygen. Such behavior is not confirmed by hybrid functional or rPT2@PBE. To demonstrate this, the DFT energy of the reaction $MgO_x + O_2 \rightarrow MgO_{x+2}$ calculated with different functionals is shown in Fig. 2. The PBE+vdW overestimation of energies at large coverages implies that, during the GA scanning, a fitness function based on PBE+vdW energy would lead to a biased sampling, because low-energy structures are different at the converged PBE0+vdW level. As can be seen in Fig. 2, for lower O_2-coverage the difference between PBE+vdW and PBE0+vdW/rPT2@PBE energies of O_2 adsorption on Mg and MgO_2 is small despite the error in the O_2 binding energy (the calculated O_2 binding energy is 6.23 eV for PBE+vdW, 5.36 for PBE0+vdW, 4.59 for rPT2@PBE, and the experimental value is 5.21 [40]). This can be explained by error cancellation for the clusters: If an O_2 molecule adsorbs non-dissociatively on Mg_MO_x, the error in the description of Mg_MO_{x+2} will cancel with the error in the description of O_2 when calculating the adsorption energy. Indeed, we find that adsorption of O_2 on Mg and MgO_2 does not lead to breaking of O-O bonds. The difference between PBE+vdW and PBE0+vdW energies of O_2 adsorption on MgO for $\mathcal{M} = 3$ is due to the difference in the description of the singlet state of MgO itself. For clusters with $x \geq 5$, correction of the O_2 binding energy error increases the difference between PBE+vdW and PBE0+vdW/rPT2@PBE adsorption energies (see the Suppl. Material). The tendency of PBE (and, as a consequence, of PBE+vdW) to overbind O_2 molecules at high coverage holds also at larger M (see the Suppl. Material).

At given T, p_{O_2}, and M, the stable stoichiometry of a Mg_MO_x cluster is determined via *ai*AT, i.e., by minimizing the Gibbs free energy of formation [19, 41]: $\Delta G_f(T, p_{O_2}) = F_{Mg_MO_x}(T) - F_{Mg_M}(T) - x\mu_O(T, p_{O_2})$. Here, $F_{Mg_MO_x}(T)$ and $F_{Mg_M}(T)$ are the Helmholtz free energies of the Mg_MO_x and the pristine Mg_M cluster (at their ground state with respect to geometry and spin), respectively, and $\mu_O(T, p_{O_2})$ is the chemical potential of oxygen. As explained in [19, 41], $F_{Mg_MO_x}(T)$ and $F_{Mg_M}(T)$ are calculated using DFT information and are expressed as the sum of DFT total energy, DFT vibrational free energy in the harmonic approximation, as well as translational, rotational, symmetry- and spin-degeneracy free-energy contributions. The dependence of μ_O on T and p_{O_2} is calculated using the ideal (diatomic) gas approximation with the same DFT functional as for the clusters [19]. The phase diagram for a particular M is constructed by identifying the lowest free-energy structures at each (T, p_{O_2}). As a representative example, we show in Fig. 3 the phase diagram for $M = 4$. Phase diagrams based on reaxFF, PBE+vdW, PBE0 (without vdW), and rPT2@PBE can be found in the Suppl. Material. We find that at all DFT levels, the phase diagrams are qualitatively and quantitatively very similar for $T > 200$ K and $p_{O_2} < 10^{-5}$ atm. For higher pressures and/or lower temperatures, however, PBE+vdW predicts larger x in Mg_MO_x as thermodynamically more stable, compared to PBE0+vdW and rPT2@PBE. This is consistent with the results shown in Fig. 2, i.e., PBE tends to favor adsorption of a larger number of O_2 molecules. PBE0 and PBE0+vdW yield almost identical phase diagrams. Thus, at the considered cluster sizes the vdW interactions within the scheme

of Ref. [32] do not play a crucial role. ReaxFF-based diagrams are very different from DFT-based ones and no conclusions, even qualitative, can be drawn from the analysis of the reactive force field results. Furthermore, we find [19] that neglecting translational, rotational, and vibrational, symmetry- and spin-degeneracy-related free-energy contributions results only in slight changes in the phase diagrams, comparable to the differences between PBE0+vdW and rPT2@PBE diagrams, for all considered M.

We have constructed phase diagrams for $1 \leq M \leq 10$. At thermodynamic equilibrium in a wide range around normal conditions, small Mg_MO_x clusters ($M \leq 5$) are found to be preferentially non-stoichiometric ($x > M$). For sizes $M = 6$, 7 we observe a competition between stoichiometric and non-stoichiometric stable structures, while for sizes $M \geq 8$ the stoichiometric composition is the most stable, with the energy gap between the stoichiometric and non-stoichiometric structures increasing with size M. In Fig. 1, we also report the relative stability of stoichiometric and non-stoichiometric structures at low ($T = 100$ K) and high ($T = 1\,000$ K) temperatures. The relative stability of stoichiometric structures increases with temperature. We also find (see Suppl. Material) that lowering p_{O_2} shifts the equilibrium towards stoichiometric structures.

In Fig. 1, we report also the spin multiplicity $\mathcal{M}$ of the low-free-energy structures. We find that in general Mg_MO_x non-stoichiometric clusters have several near-degenerate (within $\sim$0.05 eV) electronic states with different spin. The highest multiplicity we find is $\mathcal{M} = 7$ for the case Mg_4O_{12}, and values of $\mathcal{M} = 3$ and 5 are largely represented. The analysis of the spin-density shows that the unpaired electron density is localized on O_2 and O_3 moieties (see examples in the Suppl. Material). The orbitals occupied by the different unpaired electrons in the same cluster have vanishing overlaps due to large separation. The different spin-states for each isomer can be formed and coexist in oxygen atmosphere without violating spin conservation rules, since successive adsorption and desorption of the (triplet) O_2 molecules in the gas phase allows the clusters to reach all the stable spin-multiplicities observed for each cluster. The thermodynamically favored access of oxygen in small clusters is in sharp contrast to bulk pristine MgO, where stoichiometric composition is strongly favored. In all these clusters, the coordination of O atoms to Mg is maximum two. When the number of Mg is increased such that every O atom can be coordinated to three or more Mg, and at the same time the clusters have large HOMO-LUMO gap (i.e., all valence Mg electron are transferred to O_x), then stoichiometric clusters become thermodynamically stabilized.

All the quasi-degenerate spin states are populated at finite temperature, thus all the non-stoichiometric clusters with energetically quasi-degenerate states are paramagnetic. In contrast to non-stoichiometric clusters, we find that stoichiometric structures are always singlet, separated from the higher-multiplicity states by at least 1 eV. Thus, the stoichiometric clusters are diamagnetic. By looking at Fig. 3, we note that in the range of realistically achievable pressures encompassed by the rectangle, non-stoichiometric (paramagnetic) structures are thermodynamically more stable at lower temperatures, while at higher temperatures the stoichiometric (diamagnetic) structures become more stable. The temperature at which this transition occurs is a rapidly varying function of p_{O_2}. We have thus identified a class of systems that undergo an unusual paramagnetic-diamagnetic transition induced by T and p of the reactive atmosphere, where the change in magnetic behavior reflects the change in composition. All the cluster sizes we have studied present this transition, but only for sizes $3 \leq M \leq 8$ the transition is predicted to happen in the pressure range 1 Pa $\leq p_{O_2} \leq 1$ atm. The transition between paramagnetic and diamagnetic behavior is smooth when environmental conditions are changed smoothly, because different stoichiometries always coexist within few k_BT. In fact, the sand-colored areas in Fig. 3 are the regions where the free energies of the competing compositions/structures are within $2k_BT$.

In conclusion, we have presented a theoretical framework for predicting structure and stoichiometry of stable and metastable clusters in thermodynamic equilibrium with a gas atmosphere. A massively-parallel cascade genetic algorithm, i.e., an efficient scan of the potential energy of the clusters with various compositions, is combined with *ab initio* atomistic thermodynamics, a tool for evaluating the relative free energy of structures by knowing their electronic energy, vibrational frequencies, and structural parameters for the evaluation of translational and rotational entropy. The methodology has been applied to Mg clusters in an oxygen atmosphere. We have shown that small alkaline earth metal clusters form thermodynamically stable non-stoichiometric "nano-oxides", which have been overlooked so far. They are also predicted to have peculiar (p, T)-dependent, magnetic properties.

We acknowledge the cluster of excellence "Unifying Concepts in Catalysis" (UniCat, sponsored by the DFG and administered by the TU Berlin) for financial support.

[1] E. Roduner, Chem. Soc. Rev. **35**, 583 (2006).
[2] K. G. Caulton, M. G. Thomas, B. A. Sosinsky, and E. L. Muetterties, Proc. Natl. Acad. Sci. USA **73** (1976).
[3] K. Kwapien, M. Sierka, J. Dobler, J. Sauer, M. Haertelt, A. Fielicke, and G. Meijer, Angew. Chem. Int. Ed. **50**, 1716 (2011).
[4] N. Marom, M. Kim, and J. R. Chelikowsky, Phys. Rev. Lett. **108**, 106801 (2012).

[5] Y. Gao, N. Shao, Y. Pei, Z. Chen, and X. C. Zeng, ACS Nano **5**, 7818 (2011).

[6] Yimin Li *et. al.*, J. Am. Chem. Soc. **133**, 13527 (2011).

[7] W. A. Saunders, Phys. Rev. B **37**, 6583 (1988).

[8] T. Uchino, T. Yoko Phys. Rev. B **85**, 012407 (2012).

[9] P. J. Ziemann and A. W. Castleman, Jr., Phys. Rev. B **44**, 6488 (1991).

[10] C. Roberts, R.L. Johnston, Phys. Chem. Chem. Phys. **3**, 5024 (2001).

[11] M. Haertelt, A. Fielicke, G. Meijer, K. Kwapien, M. Sierkaz and J. Sauer, Phys. Chem. Chem. Phys., **14**, 2849 (2012).

[12] A. Jain, V. Kumar, M. Sluiter, and Y. Kawazoe, Comp. Mater. Sc. **36**, 171 (2006).

[13] M.-J. Malliavin, C. Coudray, J. Chem. Phys. **106**, 2323 (1997).

[14] J.M. Recio, R. Pandey, Phys. Rev. A **47**, 2075 (1993).

[15] E. de la Puente, A. Aguado, A. Ayuela, J.M. Lopez, Phys. Rev. B **56**, 7607 (1997).

[16] R. L. Johnston, Dalton Trans. **22**, 4193 (2003).

[17] M. Sierka, Progress in Surface Science **85**, 398 (2010).

[18] L. B. Vilhelmsen and B. Hammer, Phys. Rev. Lett. **108**, 126101 (2012).

[19] S. Bhattacharya, S. V. Levchenko, L. M. Ghiringhelli, M. Scheffler, to be submitted (2013).

[20] D. M. Deaven and K. M. Ho, Phys. Rev. Lett., **75**, 288 (1995).

[21] C. M. Weinert and M. Scheffler, in Defects in Semiconductors, edited by H. J. von Bardeleben (Mat. Sci. Forum 1012, 1986), pp. 2530.

[22] M. Scheffler and J. Dabrowski, Phil. Mag. A **58**, 107 (1988).

[23] K. Reuter and M. Scheffler, Phys. Rev. B **65**, 035406 (2001). Erratum: Phys. Rev. B **75**, 049901(E) (2007).

[24] K. Reuter, C. Stampfl, and M. Scheffler, in Handbook of Materials Modeling (2005 Springer), edited by S. Yip, pp. 149194.

[25] E. C. Beret, L. M. Ghiringhelli, and M. Scheffler, Faraday Discuss. **152**, 153 (2011).

[26] A.C.T. van Duin, S. Dasgupta, F. Lorant and W. A. Goddard, J. Phys. Chem. A **105**, 9396 (2001).
The reaxFF parameters for Mg and O [27] were fit [27] to a quantum-mechanics training set including MgO−bulk and O_2−molecule properties. We checked that this parametrization yields for bulk MgO lattice constant within 1 % and bulk modulus within 10 % from the experimental values; similarly, for the MgO and O_2 dimer, it gives bond length and vibrational frequency within 1 % and 10% from the respective reference values. On this set of properties, reaxFF performs remarkably well, comparable to PBE+vdW [33], PBE0+vdW [34], and HSE06+vdW [37], but it fails very clearly for small clusters.

[27] R. Zhu, F. Janetzko, Y. Zhang, A. C. T. van Duin, W. A. Goddard and D. R. Salahub, Theor. Chem. Account, **120** 479 (2008).

[28] E. Marinari, G. Parisi, Europhys. Lett. **19**, 451 (1992).

[29] D. J. Sindhikara, D. J. Emerson, and A. E. Roitberg, J. Chem. Theory Comput. **6**, 2804 (2010).

[30] A two-level GA was proposed in Ref. [18], however our cascade approach is developed into a wider scheme. Furthermore, a careful benchmark and motivation of all substeps is discussed in Ref. [19].

[31] V. Blum, R. Gehrke, F. Hanke, P. Havu, V. Havu, X. Ren, K. Reuter, and M. Scheffler, Comp. Phys. Comm. **180**, 2175 (2009).

[32] A. Tkatchenko and M. Scheffler, Phys. Rev. Lett. **102**, 073005 (2009).

[33] J. P. Perdew, K. Burke, and M. Ernzerhof, Phys. Rev. Lett. **77**, 3865 (1996). Erratum: J. P. Perdew, K. Burke, and M. Ernzerhof, Phys. Rev. Lett. **78**, 1396 (1997).

[34] J. P. Perdew, K. Burke, and M. Ernzerhof, Phys. Rev. Lett. **77**, 3865 (1996).

[35] The difference in binding energy between an isomer optimized with PBE0+vdW forces (tight / tier 1 / forces converged to 10^{-5} eV/Å), and the same isomer optimized with PBE+vdW (tight / tier 2 / forces converged to 10^{-5} eV/Å), when the energy of both geometries is evaluated via PBE0+vdW (tight / tier 2), is small, i.e., at most 0.04 eV among all cases we checked. Thus, the computational cost of the PBE0+vdW further optimization is not justified (we estimated a gain of up to a factor 2 of overall computational time just by skipping the latter optimization).

[36] N. Richter *et al.*, to be submitted (2013).

[37] A. V. Krukau, O. A. Vydrov, A. F. Izmaylov, and G. E. Scuseria, J. Chem. Phys. **125**, 224106 (2006).

[38] X. Ren, A. Tkatchenko and M. Scheffler, Phys. Rev. Lett. **106**, 153003 (2011). X. Ren, P. Rinke, C. Joas, and M. Scheffler, J. Mater. Sci. **47**, 7447 (2012).

[39] rPT2@PBE energies were calculated with FHI-aims, using "really tight" grid settings and "tier 4" basis set, and were counterpoise-corrected for the basis set superposition error.

[40] Chase Jr., M. W., NIST-JANAF Tables "4th ed.", J. Phys. Chem. Ref. Data Monogr. 9, Suppl. 1 (1998). Zero-point energy correction taken from Huber, K. P. and Herzberg, G., in *Molecular Spectra and Molecular Structure: Constants of Diatomic Molecules* (Van Nostrand Reinhold, New York, 1979), Vol. 4.

[41] E. C. Beret, M. van Wijk, L. M. Ghiringhelli, and M. Scheffler. To be submitted (2013).